intervene in MD plasticity by mediating the strengthening of active inputs. The existing information allows envisioning two mechanisms by which ERK could exert its actions on activity-dependent synapse strengthening. First, phosphorylated ERK could, at synaptic level, modulate the activity of substrates important for plasticity such as synaptic proteins (*22*), ionic channels (*23*), or adhesion molecules (*24*). A second mode of action involves translocation of phosphorylated ERK to the nucleus where it activates, directly or through kinases of the p90 ribosomal S6 kinase family, various transcription factors crucial for plasticity (*25*, *26*).

References and Notes

1. N. Berardi, T. Pizzorusso, L. Maffei, *Curr. Opin. Neurobiol.* **10**, 138 (2000).
2. T. K. Hensch *et al.*, *Science* **282**, 1504 (1998).
3. M. Fagiolini, T. K. Hensch, *Nature* **404**, 183 (2000).
4. E. M. Quinlan, B. D. Philpot, R. L. Huganir, M. F. Bear, *Nature Neurosci.* **2**, 352 (1999).
5. S. Glazewski, K. P. Giese, A. Silva, K. Fox, *Nature Neurosci.* **3**, 911 (2000).
6. C. Lodovichi, N. Berardi, T. Pizzorusso, L. Maffei, *J. Neurosci.* **20**, 2155 (2000).
7. A. K. McAllister, L. C. Katz, D. C. Lo, *Annu. Rev. Neurosci.* **22**, 295 (1999).
8. Z. J. Huang *et al.*, *Cell* **98**, 739 (1999).
9. T. Pizzorusso, G. M. Ratto, E. Putignano, L. Maffei, *J. Neurosci.* **20**, 2809 (2000).
10. S. S. Grewal, R. D. York, P. J. Stork, *Curr. Opin. Neurobiol.* **9**, 544 (1999).
11. G. E. Schafe *et al.*, *J. Neurosci.* **20**, 8177 (2000).
12. S. Blum, A. N. Moore, F. Adams, P. K. Dash, *J. Neurosci.* **19**, 3535 (1999).
13. D. E. Berman, S. Hazvi, K. Rosenblum, R. Seger, Y. Dudai, *J. Neurosci.* **18**, 10037 (1998).
14. C. M. Atkins, J. C. Selcher, J. J. Petraitis, J. M. Trzaskos, J. D. Sweatt, *Nature Neurosci.* **1**, 602 (1998).
15. Web figures 1 through 4 and text on methods are available at *Science* Online at www.sciencemag.org/cgi/content/full/292/5525/2337/DC1.
16. S. P. Davies, H. Reddy, M. Caivano, P. Cohen, *J. Biochem.* **351**, 95 (2000).
17. A. Kirkwood, M. F. Bear, *J. Neurosci.* **14**, 1634 (1994).
18. A. Kirkwood, H. K. Lee, M. F. Bear, *Nature* **375**, 328 (1995).
19. For each animal the bias of the ocular dominance distribution towards the contralateral eye was calculated using a CBI. CBI = {[N(1) – N(7)] + 1/2[N(2/3) – N(5/6)] + N(tot)}/2N(tot), where N(tot) is the total number of recorded cells and N(i) is the number of cells in class (i).
20. D. Birch, G. H. Jacobs, *Vision Res.* **19**, 933 (1979).
21. M. Fagiolini, T. Pizzorusso, N. Berardi, L. Domenici, L. Maffei, *Vision Res.* **34**, 709 (1994).
22. J. N. Jovanovic *et al.*, *Proc. Natl. Acad. Sci. U.S.A.* **93**, 3679 (1996).
23. J. P. Adams *et al.*, *J. Neurochem.* **75**, 2277 (2000).
24. C. H. Bailey *et al.*, *Neuron* **18**, 913 (1997).
25. T. A. Pham, S. Impey, D. R. Storm, M. P. Stryker, *Neuron* **22**, 63 (1999).
26. A. J. Silva, J. H. Kogan, P. W. Frankland, S. Kida, *Annu. Rev. Neurosci.* **21**, 127 (1998).

27. Supported by Ministero Universita e della Ricerca Scientifica e Tecnologica Cofinanziamento, CNR targeted project in Biotechnology SP-5, Progetto Strategico Neuroscienze, and Progetto Telethon 934.

17 January 2001; accepted 9 May 2001

Intracellular Anions as the Voltage Sensor of Prestin, the Outer Hair Cell Motor Protein

Dominik Oliver,[1] David Z. Z. He,[2] Nikolaj Klöcker,[1] Jost Ludwig,[1] Uwe Schulte,[1] Siegfried Waldegger,[3] J. P. Ruppersberg,[1] Peter Dallos,[4] Bernd Fakler[1]*

Outer hair cells (OHCs) of the mammalian cochlea actively change their cell length in response to changes in membrane potential. This electromotility, thought to be the basis of cochlear amplification, is mediated by a voltage-sensitive motor molecule recently identified as the membrane protein prestin. Here, we show that voltage sensitivity is conferred to prestin by the intracellular anions chloride and bicarbonate. Removal of these anions abolished fast voltage-dependent motility, as well as the characteristic nonlinear charge movement ("gating currents") driving the underlying structural rearrangements of the protein. The results support a model in which anions act as extrinsic voltage sensors, which bind to the prestin molecule and thus trigger the conformational changes required for motility of OHCs.

Electromotility of OHCs (*1*, *2*) occurs at acoustic frequencies and is assumed to produce the amplification of vibrations in the cochlea that enables the high sensitivity and frequency selectivity of the mammalian hearing organ (*3*, *4*). This motility results from a protein in the OHC basolateral membrane that undergoes a structural rearrangement in response to changes in the transmembrane voltage (*5*–*7*). Coupling of motility and transmembrane voltage is mediated by a charged voltage sensor within the protein that moves through the electrical field and thus gives rise to a gating current similar to that observed in voltage-gated ion channels (*8*, *9*). Recently, the gene coding for an integral membrane protein of OHCs termed prestin (Fig. 1A) has been identified (*10*). Upon heterologous expression, the protein reproduces all hallmarks of the motor protein including voltage-dependent charge movement and cell motility (*10*–*13*). Because of its fundamental role in OHC electromotility, we examined the mechanism underlying the voltage sensitivity of prestin.

Functionality of the voltage sensor of prestin was probed by measuring the nonlinear capacitance (C_{nonlin}) arising from its gating currents with the phase-tracking technique (*14*). Prestin-expressing CHO cells exhibited a bell-shaped C_{nonlin} in response to the transmembrane voltage ramped from –130 mV to 60 mV (Fig. 1B). This electrical signature was well fitted with the derivative of a first-order Boltzmann function [Eq. 1 in (*14*)] yielding values for $V_{1/2}$ and α of –75.5 ± 9.1 mV and 35.5 ± 2.3 mV (n = 16), respectively.

In contrast, no C_{nonlin} was observed in cells expressing SLC26A6 (*15*) (n = 12), another member of the family of pendrin-related transporters that exhibits closest homology to prestin (~40% identity). It is thus likely that the voltage sensor of prestin is made up of a charged residue present in the prestin sequence but absent in SLC26A6. We mutated each of the nonconserved negatively or positively charged residues in the putative membrane domain of the prestin molecule to a neutral amino acid, glutamine or asparagine, either individually or in groups [(*16*) and Fig. 1A]. In no case was the electrical signature of the voltage sensor abolished, although in some prestin mutants C_{nonlin} was shifted along the voltage axis by up to 100 mV (Fig. 1, B and C). The slope factor α characterizing the voltage dependence of C_{nonlin} was not significantly different between wild type and any of the mutants tested (*17*).

These mutagenesis results led to the idea that, instead of being an intrinsic property of the prestin molecule, the voltage sensor may be a charged particle extrinsic to the protein. We thus replaced cations and anions on either side of the membrane by *N*-methyl-D-glucamine ($NMDG^+$) or tetra-ethyl-ammonium (TEA^+) and pentane-sulfonate or sulfate, respectively. C_{nonlin} of a prestin-expressing CHO cell largely decreased on reduction of the Cl^- concentration in the whole-cell recording pipette from 150 mM to 2 mM (Fig. 2, A and B). This decrease was fully reversible, as C_{nonlin} was completely restored when Cl^- was increased back to 150 mM (Fig. 2B).

[1]Department of Physiology II, University of Tübingen, 72074 Tübingen, Germany. [2]Boys Town National Research Hospital, Omaha, NE 68131, USA. [3]Centre of Pediatrics, University of Marburg, 35037 Marburg, Germany. [4]Auditory Physiology Laboratory, Department of Neurobiology and Physiology, Northwestern University, Evanston, IL 60208, USA.

*To whom correspondence should be addressed. E-mail: bernd.fakler@uni-tuebingen.de

These findings were confirmed in patches excised from rat OHCs (*18*). Removal of Cl^- from the cytoplasmic side led to a complete but reversible loss of C_{nonlin} in all inside-out patches tested (n = 15, Fig. 2C). In contrast, replacement of Cl^- on the extracellular side by sulfate or pentane-sulfonate had no detectable effect on C_{nonlin} (n = 9, Fig. 2D). Similarly, C_{nonlin} was not affected by the cation species, K^+, Na^+, $NMDG^+$, or TEA^+, present on either side of the membrane (*19*).

Next, we studied the significance of cytoplasmic Cl^- for OHC electromotility by measuring cell-length changes in response to voltage steps (*20*). With 150 mM Cl^- in the recording pipette, OHCs displayed normal length changes with amplitudes up to 1 μm (n = 8). However, no electromotility was detected with 150 mM pentane-sulfonate replacing Cl^- in the intracellular solution (n = 14; Fig. 3). After removal of cytoplasmic Cl^-, the cells remained in the contracted state (*21*).

These results indicated that intracellular Cl^- was sufficient to confer both voltage-dependent charge movement and electromotility onto prestin, most likely by acting on a binding site within the molecule. We tested various halides and small organic anions for their ability to induce C_{nonlin}. All monovalent anions tested induced voltage-dependent charge movement when applied to inside-out patches at 150 mM (Fig. 4A) with an order of Q_{max} of $I^- \approx Br^- > NO_3^- > Cl^- > HCO_3^- > F^-$, which is similar to that observed for anion-binding to pendrin and some chloride channels (*22*, *23*). The characteristics of the charge movement differed somewhat among the various anions. Although the slope values were not significantly different from that obtained with Cl^-, the $V_{1/2}$ values covered a wide range from –138.5 ± 14.4 mV (n = 5) observed for I^- to 0.0 ± 19.6 mV (n = 4) determined for F^-. In contrast, the divalent SO_4^{2-} did not induce any detectable C_{nonlin} (Fig. 2C).

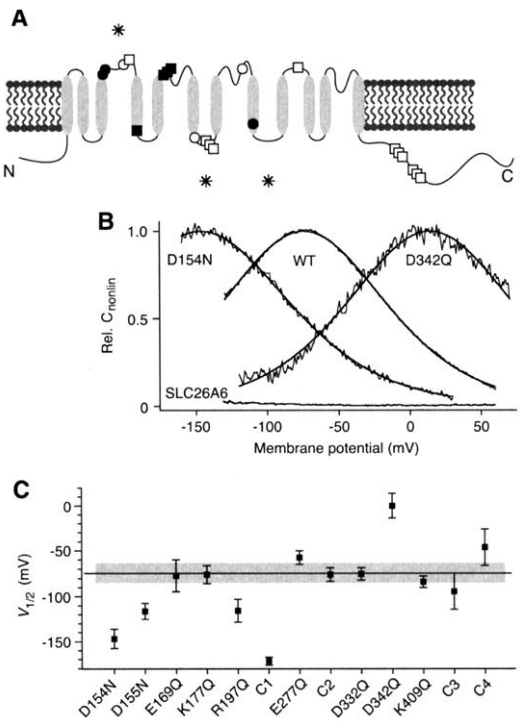

Fig. 1. Effect of neutralizing charged residues in the prestin sequence on the voltage dependence of nonlinear charge movement. (**A**) Membrane topology of prestin as suggested by hydrophobicity analysis and epitope-tagging (*28*) indicating location of the charged residues tested for involvement in the voltage sensor. Circles and squares denote negatively and positively charged amino acids, respectively; overlaid squares represent clusters of positively charged residues (C1 to C4); filling indicates significant effect on nonlinear charge movement. Asterisks mark position and location of HA tags introduced into the prestin molecule. (**B**) Relative C_{nonlin} measured in response to voltage ramps in CHO cells expressing either wild-type (WT) or mutant prestin or SLC26A6. Prestin traces are normalized to peak capacitance, and the SLC26A6 trace is scaled with respect to the WT prestin trace. Continuous lines represent fit of Eq. 1 to the prestin data [values for $V_{1/2}$ and slope (α) were −75.3 mV and 38.1 mV for WT prestin, −146.7 mV and 41.3 mV for D154N, and 14.2 mV and 38.5 mV for D342Q] (*29*). (**C**) $V_{1/2}$ values (means ± SD) determined in 5 to 10 experiments as in (B) for the prestin mutants indicated; C1 is K233Q, K235Q, and R236Q; C2 is R281Q, K283Q, and K285Q; C3 is K557Q, R558Q, and K559Q; and C4 is R571Q, R572Q, and K577Q. Continuous line and dashed area represent mean $V_{1/2}$ ± SD obtained for WT prestin.

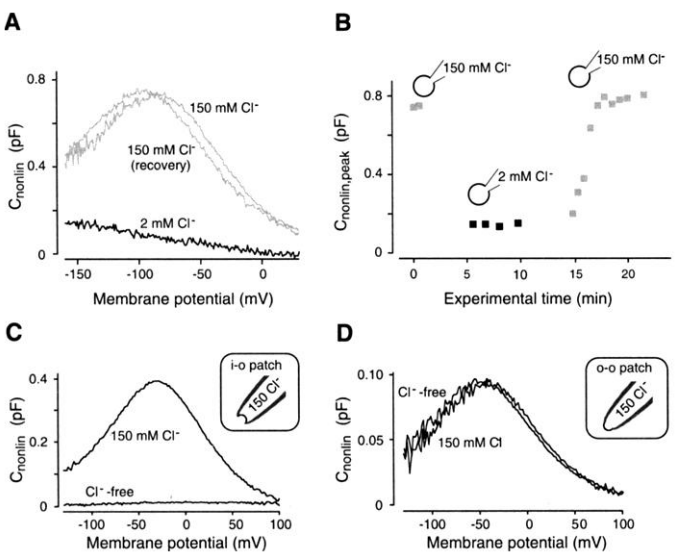

Fig. 2. Removal of Cl^- abolishes voltage-dependent charge movement of prestin in CHO cells and OHCs. (**A** and **B**) Successive whole-cell measurements of C_{nonlin} in a prestin-expressing CHO cell with alternating high and low Cl^- concentration in the recording pipette; solutions were either (millimolar concentration) 150 KCl, 10 Hepes, and 1 EGTA, or 2 KCl, 148 Na-pentane-sulfonate, 10 Hepes, and 1 EGTA. After measuring C_{nonlin} with one intracellular solution, the pipette was gently withdrawn to allow resealing of the cell before repatching with the next solution [insets in (B)]. Note the reversible decrease in C_{nonlin} when intracellular Cl^- was reduced. (**C**) C_{nonlin} measured in an inside-out patch excised from a rat OHC with and without Cl^- present at the cytoplasmic side of the patch; 150 mM Cl^- was replaced by 50 mM SO_4^{2-}. (**D**) C_{nonlin} measured in an outside-out patch excised from a rat OHC with and without Cl^- present at the extracellular side of the patch; Cl^- replacement as in (C).

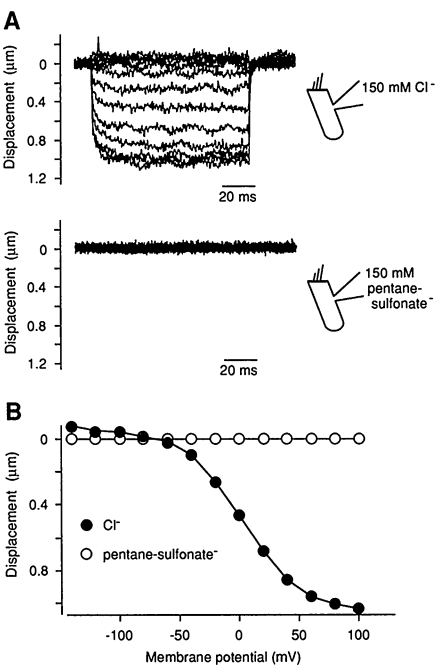

Fig. 3. Removal of Cl^- eliminates voltage-dependent motility of OHCs. (**A**) Electromotility of a gerbil OHC measured in whole-cell voltage-clamp mode with high (150 mM Cl^-; upper panel) or low Cl^- (150 mM pentane-sulfonate$^-$; lower panel) in the patch pipette. Holding potential was −70 mV, membrane potential was stepped between −140 mV and 100 mV in 20-mV step increments. Pipette solutions were (millimolar concentration): 150 KCl, 10 Hepes, and 1 EGTA, or 150 Na-pentane-sulfonate, 0.5 KCl, 10 Hepes, and 1 EGTA. (**B**) Steady-state motility-voltage relation determined from the experiments in (A).

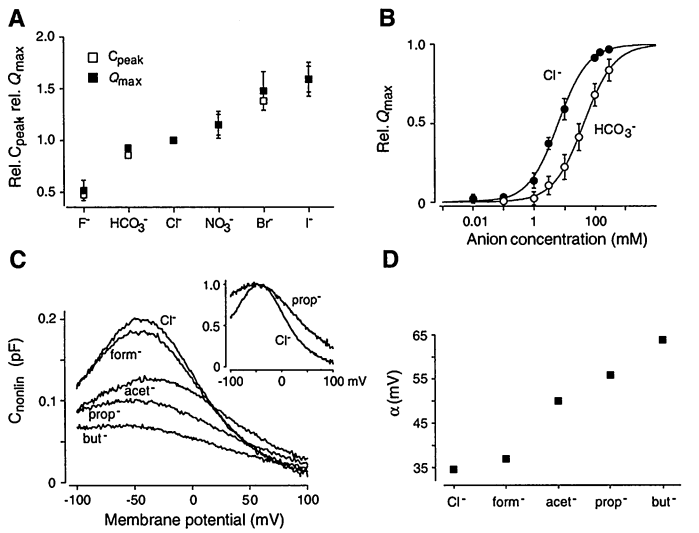

Fig. 4. Functional characteristics of the voltage sensor are determined by the anion species. (**A**) Relative peak of C_{nonlin} and Q_{max} measured in inside-out patches from rat OHCs with the anions indicated present at the cytoplasmic side of the patches. Values are means ± SD of three to seven experiments; C_{nonlin} and Q_{max} values for Cl^- were used for normalization. (**B**) Concentration-Q_{max} curves for Cl^- and HCO_3^- determined in inside-out patches from rat OHCs (*30*). Lines represent fit of a logistic function to the data (means ± SD of four to eight experiments) with values for EC_{50} and Hill coefficient of 6.3 mM and 0.89 for Cl^- and 43.6 and 0.87 for HCO_3^-, respectively. (**C**) C_{nonlin} measured in an inside-out patch from a rat OHC with Cl^- and the various carboxylic acids present at the cytoplasmic surface of the patch. Form$^-$ is formate, acet$^-$ is acetate, prop$^-$ is propionate, and but$^-$ is butyrate. (**D**) Slope (α) of C_{nonlin} determined from the experiment in (C). Note the decrease in slope with increase in chain length of the carboxylic acid.

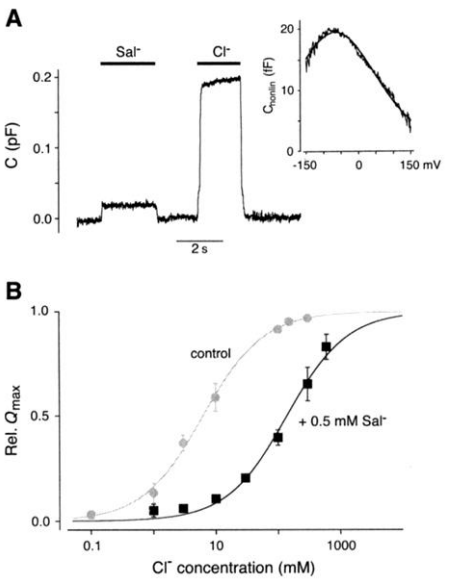

Fig. 5. Salicylate acts as a competitive antagonist at the anion-binding site. (**A**) Nonlinear capacitance induced by application of 10 mM salicylate (ionic strength maintained with 47 mM SO_4^{2-}) or 150 mM Cl^- at an inside-out patch excised from a rat OHC. Holding potential was −50 mV, applications as indicated by horizontal bars. Inset: C_{nonlin} measured in an inside-out patch from a rat OHC in response to a voltage ramp from −150 mV to 150 mV with 150 mM salicylate present at the cytoplasmic side of the patch. Continuous line represents fit of Eq. 1 to the data yielding values for $V_{1/2}$ and α of −65.3 mV and 83.3 mV, respectively. (**B**) Concentration-Q_{max} relations for Cl^- determined in inside-out patches from rat OHCs in the absence (control) and presence of 0.5 mM salicylate. Lines represent fit of a logistic function to the data (means ± SD of five to eight experiments) with values for EC_{50} and Hill coefficient of 6.3 mM and 0.89 (control) and 138.4 mM and 0.90 (presence of salicylate).

Although all halides were able to induce voltage-dependent charge movement, only Cl^- and bicarbonate (HCO_3^-) are thought to be present in the cytoplasm at millimolar concentrations. Such concentrations are indeed necessary as demonstrated in experiments measuring the affinity of prestin for both anions. The concentrations required for half-maximal charge movement were 6.3 mM and 43.6 mM for Cl^- and HCO_3^-, respectively (Fig. 4B). Together these findings suggest that Cl^- and HCO_3^- work as the voltage sensor of prestin, which is translocated when the membrane potential is changed. This view is further supported by experiments characterizing the C_{nonlin} induced by carboxylic acids of increasing chain length. Formate, acetate, propionate, and butyrate were all able to induce nonlinear charge movement when applied to inside-out patches (Fig. 4, C and D). However, although the slope of C_{nonlin} induced by formate was almost identical to that obtained with Cl^- (α was 37.5 ± 2.1 mV and 34.9 ± 2.4 mV for formate and Cl^-, respectively; $n = 3$), it decreased significantly with increasing chain length of the carboxylic acid (α for acetate, propionate, and butyrate was 51.1 ± 2.2 mV, 60.6 ± 4.1 mV, and 71.7 ± 6.9 mV; $n = 3$; see also inset Fig. 4C). Accordingly, the transmembrane voltage required for moving butyrate through the electrical field is more than twice that necessary for translocating Cl^- or formate.

These results support a model in which the intracellular anions Cl^- and HCO_3^- act as the voltage sensor of prestin (*24*). We propose that after binding to a site with millimolar affinity, these anions are translocated across the membrane by the transmembrane voltage: toward the extracellular surface upon hyperpolarization, toward the cytoplasmic side in response to depolarization. Subsequently, this translocation triggers conformational changes of the protein that finally change its surface area in the plane of the plasma membrane. The area decreases when the anion is near the cytoplasmic face of the membrane (cell contraction), it increases when the ion has crossed the membrane to the outer surface (cell elongation). As concluded from the lack of effect on exchanging anions on the extracellular side (Fig. 2D), this outer position of the voltage sensor is inaccessible from the extracellular space.

According to this model, any molecule interacting with the anion-binding site and repelling Cl^- should reduce the structural rearrangements required for cell motility. We thus performed experiments with salicylate, a membrane-permeable inhibitor of electromotility usually applied to OHCs from the extracellular side (*25*, *26*). Salicylate induced a C_{nonlin} when applied to the cytoplasmic side, indicating interaction with the anion-binding site (Fig. 5A). However, the voltage dependence of salicylate-induced C_{nonlin} was shallow, similar to that of the large carboxylic acids, and resulted in only small charge movement over the entire physiological voltage range (inset of Fig. 5A). Coapplication of 0.5 mM salicylate with Cl^- shifted the concentration-charge relation for Cl^- toward higher concentrations by more than 20-fold, indicating competition between these anions. The affinity of the anion-binding site for salicylate as calculated from this shift is about 300 times that for Cl^- [K_{Sal} = 21 μM; (*27*)]. This provides a straightforward explanation for the efficacy of salicylate in blocking OHC electromotility.

The present findings offer a molecular framework for understanding the voltage sensitivity and resulting structural changes of the OHC motor protein. Direct experimental access to anion binding and translocation makes prestin a model for investigating functionality of anion-transporting membrane proteins.

References and Notes

1. J. F. Ashmore, *J. Physiol. (London)* **388**, 323 (1987).
2. W. E. Brownell, C. R. Bader, D. Bertrand, Y. de Ribaupierre, *Science* **227**, 194 (1985).
3. P. Dallos, *J. Neurosci.* **12**, 4575 (1992).
4. G. Frank, W. Hemmert, A. W. Gummer, *Proc. Natl. Acad. Sci. U.S.A.* **96**, 4420 (1999).
5. P. Dallos, B. N. Evans, R. Hallworth, *Nature* **350**, 155 (1991).
6. K. H. Iwasa, *J. Acoust. Soc. Am.* **96**, 2216 (1994).
7. F. Kalinec, M. C. Holley, K. H. Iwasa, D. J. Lim, B. Kachar, *Proc. Natl. Acad. Sci. U.S.A.* **89**, 8671 (1992).
8. J. F. Ashmore, in *Mechanics of Hearing* J. P. Wilson, D. Kemp, Eds. (Plenum, New York, 1989), pp. 107–113.
9. J. Santos-Sacchi, *J. Neurosci.* **11**, 3096 (1991).
10. J. Zheng *et al.*, *Nature* **405**, 149 (2000).
11. I. A. Belyantseva, H. J. Adler, R. Curi, G. I. Frolenkov, B. Kachar, *J. Neurosci.* **20**, RC116 (2000) (published online 19 December 2000).

12. J. Ludwig *et al.*, *Proc. Natl. Acad. Sci. U.S.A.* **98**, 4178 (2001).
13. J. Santos-Sacchi, W. Shen, J. Zheng, P. Dallos, *J. Physiol. (London)* **531**, 661 (2001).
14. For functional expression, the COOH-terminal green fluorescent protein (GFP)–fusion construct of rat prestin (pBK-CMV-rPrestin-C_{GFP}) was injected into Chinese hamster ovary cells (CHO dhFr$^-$) as described (*12*). Whole-cell patch-clamp recordings were done at room temperature (21° to 24°C) 20 to 40 hours after injection; the Sylgard-coated quartz electrodes used had resistances of 2 to 3 MΩ when filled with a solution containing (millimolar concentration) 135 KCl, 3.5 $MgCl_2$, 0.1 $CaCl_2$, 5 K_2EGTA, 5 Hepes, and 2.5 Na_2ATP (pH adjusted to 7.3 with NaOH). Extracellular solution was (millimolar concentration) 144 NaCl, 5.8 KCl, 1.3 $CaCl_2$, 0.9 $MgCl_2$, 10 Hepes, 0.7 Na_2HPO_4, and 5.6 glucose (pH adjusted to 7.3 with KOH).
    The C_{nonlin} was measured by using a software-based lock-in technique ("phase-tracking") as described [D. Oliver, B. Fakler, *J. Physiol. (London)* **519**, 791 (1999); J. D. Herrington, K. R. Newton, R. J. Bookman, *Pulse-Control V4.7* (University of Miami, Miami, FL, 1995)]. Briefly, lock-in phase angles, yielding signals proportional to changes in C_m and conductance, were calculated by dithering the series resistance by 0.5 MΩ. Capacitance was calibrated by a 100 fF-change of the C_m-compensation setting. Command sinusoid (f = 2.6 kHz; 10 mV) was filtered at 8 kHz with an 8-pole Bessel filter, and 16 periods were averaged to generate each capacitance point. To obtain the voltage dependence of membrane capacitance, voltage ramps were summed to the sinusoid command. Capacitance was fitted with the derivative of a first-order Boltzmann function

$$C(V) = C_{lin} + \frac{Q_{max}}{\alpha e^{\frac{V - V_{1/2}}{\alpha}}\left(1 + e^{\frac{V - V_{1/2}}{\alpha}}\right)^2} \quad (1)$$

    where C_{lin} is residual linear membrane capacitance, V is membrane potential, Q_{max} is maximum voltage-sensor charge moved through the membrane electrical field, $V_{1/2}$ is voltage at half-maximal charge transfer, and α is the slope factor of the voltage dependence. Processing and fitting of data was performed with IgorPro (Wave Metrics); all data are given as means ± SD.
15. S. Waldegger *et al.*, *Genomics* **72**, 43 (2001).
16. Site-directed mutagenesis on rat prestin (pBK-CMV-rPrestin-C_{GFP}) was performed as described [U. Schulte *et al.*, *Proc. Natl. Acad. Sci. U.S.A.* **96**, 15298 (1999)] and verified by sequencing.
17. D. Oliver, B. Fakler, unpublished data.
18. Inside-out and outside-out patches were excised from the lateral cell membrane of OHCs in the intact apical coil of the cochlea, isolated from 3- to 4-week-old Wistar rats as described [D. Oliver *et al.*, *Neuron* **26**, 595 (2000)]. Patch pipettes were pulled from quartz or borosilicate glass, coated with Sylgard, and filled with a solution containing (millimolar concentration): 150 KCl, 10 Hepes, and 1 EGTA (pH adjusted to 7.3 with KOH). Pipette resistances were 1.2 to 1.8 MΩ for inside-out patches and 2 to 3 MΩ for outside-out patches. C_{nonlin} of the patch membrane was measured as described for whole-cell recordings. Lock-in phase angles were determined by C_m dithering.
    Solutions with varying anionic and cationic composition were applied to the exposed face of the patch via a gravity-fed, multi-barrel capillary. The basic composition of these solutions was (millimolar concentration): 150 Cat^+An^-, 10 Hepes, and 1 EGTA. For exchange of cations, Cat^+ was K^+, Na^+, TEA^+, or $NMDG^+$ and An^- was Cl^-. For exchange of anions, Cl^- was replaced by F^-, Br^-, I^-, NO_3^-, HCO_3^-, formate$^-$, acetate$^-$, propionate$^-$, butyrate$^-$, pentane-sulfonate$^-$, or salicylate$^-$. The cation was K^+, except for solutions containing pentane-sulfonate or salicylate, which were obtained as Na^+ salts. The pH was adjusted to 7.3 with the respective hydroxide. For HCO_3^- as the anion, a total [$KHCO_3$] of 1.1 times the free [HCO_3^-] was used, because [HCO_3^-]/([HCO_3^-] + [H_2CO_3 + CO_2]) = 0.9 at pH 7.3 (adjusted with H_2SO_4). Replacement of Cl^- by the divalent SO_4^{2-} was done either equimolarly with 150 mM K_2SO_4 or with 50 mM K_2SO_4, yielding constant ionic strength. A 3 M KCl agar bridge was used as the bath electrode to avoid drifts in electrode offsets due to changes of [Cl^-] in the bath solution. Liquid junction potentials arising from different solution composition were monitored as a shift in reversal potential of the nonselective leak current. These shifts were smaller than 20 mV and were not corrected.
19. D. Oliver, unpublished data.
20. Electromotility measurements were performed on adult gerbil OHCs isolated from the apical half of the cochlea [D. Z. Z. He, B. N. Evans, P. Dallos, *Hear. Res.* **78**, 77 (1994)] by using the whole-cell voltage-clamp configuration. Motility was measured with an electrooptical technique, whereby the cell's ciliated pole was imaged onto a photodiode through a rectangular slit [P. Dallos, B. N. Evans, R. Hallworth, *Nature* **350**, 155 (1991)]. The photocurrent was proportional to the displacement of the cell's image in the slit. Calibration of displacement was done by estimation from videotaped images. High and low Cl^- internal solutions were used in any batch of cells.
21. D. Z. Z. He, P. Dallos, unpublished data.
22. C. Fahlke, C. Durr, A. L. George, *J. Gen. Physiol.* **110**, 551 (1997).
23. D. A. Scott, L. P. Karniski, *Am. J. Physiol. Cell Physiol.* **278**, C207 (2000).
24. Supplementary material in the form of a brief movie is available on *Science* Online at www.sciencemag.org/cgi/content/full/292/5525/2340/DC1.
25. M. J. Tunstall, J. E. Gale, J. F. Ashmore, *J. Physiol. (London)* **485**, 739 (1995).
26. S. Kakehata, J. Santos-Sacchi, *J. Neurosci.* **16**, 4881 (1996).
27. The dissociation constant of salicylate, K_{Sal}, was determined from the equation $K_{Sal} = [Sal^-]/(K_{Cl,Sal}/K_{Cl} - 1)$, assuming a Hill coefficient of 1 ($K_{Cl,Sal}$ and K_{Cl} are apparent dissociation constants of Cl^- in the presence and absence of salicylate, respectively).
28. Hemagglutinin (HA) tags were introduced into the prestin sequence at positions 168, 281, and 371, and immunocytochemistry was performed on transfected opossum kidney cells as described [N. Klöcker, D. Oliver, J. P. Ruppersberg, H. G. Knauss, B. Fakler, *Mol. Cell. Neurosci.* **17**, 514 (2001)]. Immunoreactivity was imaged with a confocal laser scanning microscope.
29. Single-letter abbreviations for the amino acid residues are as follows: D, Asp; E, Glu; K, Lys; N, Asn; Q, Gln; and R, Arg.
30. For determination of concentration-Q_{max} relations, solutions contained (millimolar concentration) x KAn (An is Cl^- or HCO_3^-), 10 Hepes, 1 EGTA (pH adjusted to 7.3 with KOH for chloride solution and K_2SO_4 for bicarbonate solution). When $x < 150$ mM, ionic strength was maintained by substitution with [K_2SO_4] = (150 mM − x)/3. Values for bicarbonate are free [HCO_3^-]. Data measured in the absence of Cl^- amd HCO_3^- were substrated from capacitance traces, and Q_{max} was normalized to the value at saturating [Cl^-] for each patch. In a set of control experiments, correction for ionic strength was omitted, but osmolarity was kept constant by addition of sucrose; the respective values for EC_{50} and Hill coefficient were 6.6 mM and 1.1.
    For determination of concentration-Q_{max} relations in the presence of salicylate, data measured in 0 Cl^- + 0.5 mM salicylate were substracted from capacitance traces. Q_{max} was normalized to the value at saturating [Cl^-] in the absence of salicylate for each patch.

31. We thank J. P. Adelman and C. Fahlke for stimulating discussions, and S. Weidemann and S. Eble for excellent technical assistance. This work was supported by a grant of the Deutsche Forschungsgemeinschaft to B.F. (SFB 430/A1) and by a NIH grant to P.D. (DC00089).

22 March 2001; accepted 30 April 2001